Controlling Membrane Cholesterol Content. A Role for Polyunsaturated (Docosahexaenoate) Phospholipids†

Michael R. Brzustowicz,[‡,§,||] Vadim Cherezov,[⊥] Mustapha Zerouga,[#] Martin Caffrey,[⊥] William Stillwell,[§,#] and Stephen R. Wassall*[,‡,§]

Department of Physics, Indiana University Purdue University Indianapolis, Indianapolis, Indiana 46202-3273, Biochemistry, Biophysics, and Chemistry, The Ohio State University, Columbus, Ohio 43210-1173, Department of Biology, Indiana University Purdue University Indianapolis, Indianapolis, Indiana 46202-5132, and Medical Biophysics Program, Indiana University School of Medicine, Indianapolis, Indiana 46202-5122

Received June 11, 2002; Revised Manuscript Received August 8, 2002

ABSTRACT: The molecular organization of cholesterol in 1,2-didocosahexaenoylphosphatidylcholine (22:6-22:6PC) and 1-stearoyl-2-docosahexaenoylphosphatidylcholine (18:0-22:6PC) bilayers was investigated. Using low- and wide-angle X-ray diffraction (XRD), we determined that the solubility of the sterol at 20 °C was 11 ± 3 mol % in 22:6-22:6PC vs 55 ± 3 mol % in 18:0-22:6PC bilayers. Solubility in the dipolyunsaturated membrane rose to 17 ± 3 mol % at 40 °C, while in the saturated−polyunsaturated membrane there was no change within experimental uncertainty. We compared the molecular orientation of [3α-$^2H_1$]cholesterol incorporated into 22:6-22:6PC bilayers to its solubility limit and into 18:0-22:6PC bilayers to a comparable concentration (10 mol %) in solid-state ^2H NMR experiments. The sterol possessed a tilt angle $\alpha_0 = 24° \pm 1°$ in 22:6-22:6PC that was independent of temperature over a range from 20 to 40 °C. In contrast, the value was $\alpha_0 = 21° \pm 1°$ in 18:0-22:6 bilayers at 20 °C and increased to $\alpha_0 = 24° \pm 1°$ at 40 °C. We attribute the low solubility of cholesterol in 22:6-22:6PC membranes to steric incompatibility between the rigid steroid moiety and the highly disordered docosahexaenoic acid (DHA) chain, which has the potential to promote lateral heterogeneity within DHA-rich membranes. Considering 22:6-22:6PC to be the most unsaturated phospholipid found in vivo, this model membrane study provides a point of reference for elucidating the role of sterol−lipid interactions in controlling local compositional organization. Our results form the basis for a model that is consistent with cholesterol's ability to modulate the activity of certain neural transmembrane proteins.

DHA[1] (22:6 ω-3) is a 22-carbon PUFA with six cis double bonds located at carbons 4, 7, 10, 13, 16, and 19. Its incorporation into membrane phospholipids has profound, positive effects on human health (*1*) and is essential for neural development and function (*2*, *3*). A small body of work has accumulated which explores DHA's unique role in membrane organization as a plausible molecular rationale for the absolute necessity of this highly polyunsaturated fatty acid (*4*). From these observations, it has been suggested that phospholipids containing the polyunsaturated DHA acyl chain undergo lateral phase separation into regions containing little cholesterol. In contrast, phospholipids and sphingolipids containing saturated acyl chains phase separate into regions rich in cholesterol that have recently been referred to as rafts (*5*). The proposed existence of cholesterol-rich and cholesterol-poor domains is an attractive hypothesis for the organization and functioning of cellular membranes (*6*).

Although the mechanism for microdomain formation remains elusive, cholesterol-dependent molecular sorting of membrane lipids based upon differences in ordering for polyunsaturated vs saturated acyl chains is a promising candidate (*4*, *5*). Phospholipid−cholesterol interactions have been reviewed extensively (*7*−*9*). Order parameter profiles and phase diagrams exist for homoacid and heteroacid phospholipids containing a saturated fatty acid at the *sn*-1 position. They clearly relate acyl chain molecular order to thermodynamic properties as functions of both temperature and cholesterol concentration. The sterol acts by restricting the formation of gauche rotomers in the isomerizable C−C bonds of saturated acyl chains. For cholesterol concentrations above ∼30 mol %, the membrane is said to be in the liquid-ordered (l_o) state. This state is characterized by a predomi-

† Research supported in part by grants from the National Institutes of Health (CA 57212 to W.S. and GM 56969 and GM 61010 to M.C.) and the National Science Foundation (DIR 9016683 and DBI 9981990 to M.C.)

* Address correspondence to this author at the Department of Physics, IUPUI, 402 N. Blackford St., Indianapolis, IN 46202-3273. Tel: (317) 274-6908. Fax: (317) 274-2393. E-mail: swassall@iupui.edu.

‡ Department of Physics, Indiana University Purdue University Indianapolis.

§ Medical Biophysics Program, Indiana University School of Medicine.

|| Present address: Department of Molecular and Cellular Physiology, Stanford University, Stanford, CA 94305-5489.

⊥ Biochemistry, Biophysics, and Chemistry, The Ohio State University.

Department of Biology, Indiana University Purdue University Indianapolis.

[1] Abbreviations: DHA, docosahexaenoic acid; AA, arachidonic acid; l_d, liquid disordered; l_o, liquid ordered; nAchR, nicotinic acetylcholine receptor; PUFA, polyunsaturated fatty acid; ROS, rod outer segment; XRD, X-ray diffraction; 22:6-22:6PC, 1,2-didocosahexaenoyl-*sn*-phosphatidylcholine; 18:0-22:6PC, 1-stearoyl-2-docosahexaenoyl-*sn*-phosphatidylcholine; 20:4-20:4PC, 1,2-diarachidonoyl-*sn*-phosphatidylcholine; 18:0-20:4PC, 1-stearoyl-2-arachidonoyl-*sn*-phosphatidylcholine.

10.1021/bi0262808 CCC: $22.00
Published on Web 09/20/2002

nance of trans rotomeric states in the saturated acyl chain, somewhat akin to the gel phase, but with rapid axial rotation about the bilayer normal and a high degree of lateral mobility similar to that within the liquid-disordered (l_d) phase (*10*). The l_d phase is formed at lower sterol content and is synonomous with the conventional lamellar liquid-crystalline (L_α) phase, characterized by extensive trans/gauche isomerization along the chain and rapid rotational and translational motions. Elucidation of the ordering and dynamics of polyunsaturated acyl chains only began in earnest over the past decade or so, and little is known about the interaction between polyunsaturated phospholipids and cholesterol (*4*). Recent molecular dynamics (MD) simulations confirm that the repeated −C=C−C−C=C− structural motif in polyunsaturated acyl chains confers greater conformational flexibility than within saturated chains (*11*−*13*), while the impact of cholesterol on PUFA conformation and dynamics has yet to be tackled. The problem is particularly complex for DHA, the most unsaturated acyl chain found in vivo.

Phospholipids in vivo typically contain a saturated acyl moiety at the *sn*-1 position and an unsaturated acyl moiety at the *sn*-2 position (*7*). Neural tissues with an abundance of *sn*-1, *sn*-2 dipolyunsaturation are an exception, particularly retinal membranes where phospholipid species such as 22:6-22:6PC have been isolated (*14*). We have shown previously that l_d phases comprising polyunsaturated AA (20:4 ω6) acyl chains with four cis double bonds at both the *sn*-1 and *sn*-2 positions do not accommodate high levels of cholesterol into the membrane (*15*, *16*). Our solid-state ^{2}H NMR and XRD studies examined 20:4-20:4PC vs 18:0-20:4PC bilayers where more than 3-fold lower solubility to sterol was observed for the dipolyunsaturated system. We interpreted this reduction as a molecular rationale for cholesterol's exclusion from highly polyunsaturated environments within membranes of heterogeneous composition. The concentration of AA, however, is less than DHA in neural membranes where the majority of arachidonate is typically esterified to a sparse population of phosphatidylinositol (PI) (*14*, *17*−*19*). In contrast, DHA is the most common acyl moiety esterfied to phosphatidylethanolamine (PE) and phosphatidylserine (PS) in both synaptic vesicle membranes (*17*) and nAchR-rich postsynaptic membranes (*18*), while in retinal ROS disk membranes DHA appears primarily esterified to phosphatidylcholine (PC) (*19*). Synaptic tissues are also rich in cholesterol, containing as high as ∼40 mol % for the examples cited above (*17*, *18*). The concentration is lower (<20 mol %) in ROS membranes and, not suprisingly, decreases as the DHA content increases for distally mobile ROS disks (*19*). Although previous evidence has suggested a marked incompatibility between cholesterol and DHA (*20*), the molecular organization of the sterol in DHA-rich membranes has not yet been studied.

Here we extend the biological relevance of our earlier work with AA-containing membranes by observing the molecular organization of cholesterol in model membranes comprised of the more highly polyunsaturated DHA. We compare the behavior of the sterol in 22:6-22:6PC and 18:0-22:6PC membranes. First, using ^{31}P NMR and XRD, we establish that only lamellar phase was formed under the conditions of our investigation, since it has been previously noted that dipolyunsaturated PC systems may form nonbilayer phases (*21*, *22*). We next utilize XRD to determine the maximum amount of cholesterol that can be intercalated into 22:6-22:6PC bilayers relative to control 18:0-22:6PC bilayers. ^{2}H NMR is then employed to probe the molecular ordering, i.e., most probable orientation, of deuterated [3α-$^2H_1$]cholesterol as modulated by polyunsaturation. In this work we demonstrate convincingly that a significant difference exists between the molecular organization of cholesterol in 22:6-22:6PC and 18:0-22:6PC bilayers. We discuss our results in relation to previous observations on less unsaturated membranes. The view that emerges from our research is that cholesterol is discriminated against in highly unsaturated environments and that PUFA play a crucial role in establishing heterogeneity in the lateral organization of membranes. Finally, we present a model for neural membrane organization which is consistent with cholesterol's ability to activate nAchR and to inhibit rhodopsin (*23*).

EXPERIMENTAL PROCEDURES

Materials. Avanti Polar Lipids (Alabaster, AL) was the source of 18:0-22:6PC and 22:6-22:6PC. Additional 22:6-22:6PC was synthesized according to Zerouga et al. (*24*). The starting materials for the synthesis, L-α-glycerophosphorylcholine and DHA, were purchased from Sigma (St. Louis, MO) and Nu-Chek Prep, Inc. (Elysian, MN), respectively. Cholesterol deuterated at the 3α position, [3α-$^2H_1$]-cholesterol, was synthesized by the reduction of 5-cholesten-3-one with lithium aluminum deuteride ($LiAl^2H_4$) according to Oldfield et al. (*25*). The chemicals for this synthesis were bought from Steraloids (Newport, RI) and Sigma, respectively. Cholesterol, which was subsequently recrystalized from hot ethanol, and butylated hydroxytoluene (BHT) were purchased from Sigma. Isotec Inc. (Miamisburg, OH) was the source of deuterium-depleted water (DDW).

All lipids showed a single spot by thin-layer chromatography (TLC) and were used without further purification. By adhering strictly to the precautions outlined below, DHA-containing samples showed only one spot on TLC after experiments at 20−40 °C lasting 1−3 days.

Sample Preparation. Because of the sensitivity of polyunsaturated phospholipids to oxidation, all sample preparation was carried out under a stream of nitrogen or in a nitrogen atmosphere within a home-built glovebox, and exposure to light was minimized. Milli-Q water, DDW, and buffer were thoroughly degassed.

Stock solutions of lipids dissolved in chloroform were combined in an appropriate ratio, and the antioxidant BHT in degassed methanol was added (1:250 mol of BHT relative to PC). For NMR and XRD experiments the total dry weight of the lipid was ∼100 and ∼10 mg, respectively. Organic solvent was evaporated under a gentle stream of nitrogen gas. The sample was then taken up in a small amount (∼200 μL) of cyclohexane and frozen in liquid nitrogen. Subsequent vacuum pumping at 10 mTorr for ∼20 h ensured the removal of bulk and trace solvent from the sample which was kept frozen with dry ice. The resultant fluffy white powders were allowed to warm to room temperature and were vortex mixed with 50 wt % 50 mM Tris buffer (pH 7.5). The pH was corrected with dilute (10^{-2}−10^{-4} M) NaOH following the addition of ∼1 mL of degassed Milli-Q water (XRD samples) or degassed DDW (NMR samples). After a single lyophilization, samples for XRD experiments were hydrated to 50 wt

% with Milli-Q water. The resultant multilamellar dispersions were transferred to 1 mm o.d. quartz capillary tubes (Charles Supper Co., Natick, MA), centrifuged for ~5 min to pellet the sample, and sealed (*16*). Prior to final hydration with 50 wt % DDW, five additional cycles of lyophilization with excess DDW (500 μL) were performed with samples for ^{2}H NMR experiments to reduce the signal from residual ^{2}HHO. The resultant multilamellar dispersions were transferred to 5 mm glass NMR tubes and sealed with a Teflon cap or Teflon-coated plug. All samples were stored at −80 °C and were equilibrated at room temperature for ~1 h prior to experimentation.

X-ray Diffraction. The solubility of cholesterol in a membrane was determined by XRD (*16*). Cholesterol, in excess of the solubility limit, phase separates from membranes and forms monohydrate crystals which may be quantified by detecting the associated, characteristic second-order diffraction peaks (*16*, *26*, *27*). Their respective reciprocal and real spacings are (002) 0.3701 Å^{-1}, 17.0 Å; (020) 1.033 Å^{-1}, 6.079 Å; and (200) 1.044 Å^{-1}, 6.015 Å (*28*). The combined integrated intensities of these reflections (normalized with respect to the integrated intensity of the lipid wide-angle peak) were then plotted against the total concentration of cholesterol added. Linear extrapolation to zero intensity was used to give cholesterol solubility, χ_{chol}^{XRD}, usually with better than ±3 mol % accuracy.

The observation of sharp first- and second-order lamellar diffraction peaks at low angle was taken as evidence that samples were in the lamellar phase. The lamellar repeat spacing (d_{100}) was typically 70 Å.

Solid-State NMR. The molecular orientation of [3α-^{2}H$_1$]-cholesterol intercalated into membranes was observed by solid-state ^{2}H NMR spectroscopy (*16*). Powder pattern spectra were collected at 27.6 MHz on a home-built spectrometer (*29*) using the quadrupolar echo sequence (90°$_x$−τ−90°$_y$−acquire−delay)$_n$ (*30*). Spectral parameters were data set size = 1K, pulse width = 3−4 μs, τ = 75 μs, sweep width = ±500 kHz, delay = 75 ms, and number of acquisitions n = 50000−100000.

The dominant peaks of the ^{2}H NMR powder pattern for [3α-^{2}H$_1$]cholesterol incorporated into multilamellar dispersions have residual quadrupolar splitting

$$\Delta\nu_r = \frac{3}{4}\left(\frac{e^2qQ}{h}\right)|S_{CD}| \quad (1)$$

where e^2qQ/h = 170 kHz is the static quadrupolar coupling constant and S_{CD} is the order parameter describing the angular fluctuations undergone by the 3α C−^{2}H bond as the sterol reorients rapidly about the bilayer normal (*15*, *16*, *25*, *31*). The order paremeter may be written as the product

$$S_{CD} = S_\alpha S_\gamma \quad (2)$$

The latter term S_γ (=−0.455) is a geometric factor determined by the angle γ (=79°) between the C−^{2}H bond vector and the long molecular axis of the rigid steroid moiety (*32*), while the former term S_α is the molecular order parameter describing the wobbling of the long molecular axis relative to the bilayer normal. S_α was calculated from experimentally observed splittings $\Delta\nu_r$ according to eqs 1 and 2. Assuming an axially symmetric Gaussian distribution of angles, α, applies to the wobbling motion, numerical integration of

$$S_\alpha = \frac{\frac{1}{2}\int_0^\pi \sin\alpha \exp(-\alpha^2/2\alpha_0^2)(3\cos^2\alpha - 1)\,d\alpha}{\int_0^\pi \sin\alpha \exp(-\alpha^2/2\alpha_0^2)\,d\alpha} \quad (3)$$

then gave the most probable orientation α_0 (tilt angle) of the steroid moiety within the membrane (*15*, *16*, *25*, *31*).

Verification that samples were in the lamellar phase was obtained from the characteristic shape of their ^{1}H-decoupled ^{31}P NMR spectra (*33*). The spectra were collected at 72.9 MHz using the spin−echo sequence (90°$_x$−τ−180°$_y$−acquire−delay)$_n$ (*34*). Spectral parameters were data set size = 2K, pulse width (90°) = 3−4 μs, τ = 200 μs, sweep width = ±25 kHz, delay = 1.0 s, and number of acquisitions n = 2000.

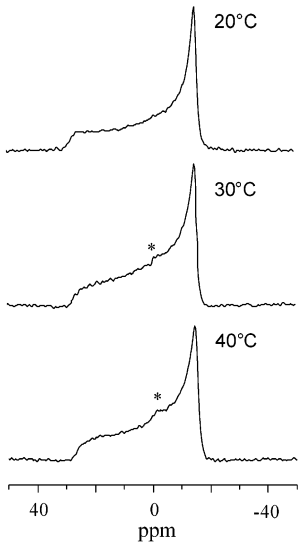

FIGURE 1: ^{1}H-decoupled ^{31}P NMR spectra for 50 wt % aqueous multilamellar dispersions containing 22:6-22:6PC/50 mol % cholesterol in 50 mM Tris (pH 7.5) at 20, 30, and 40 °C. Spectral parameters were as described in the text. An asterisk denotes a small isotropic peak in the spectra acquired at 30 and 40 °C.

RESULTS

^{31}P NMR. ^{31}P NMR was used to establish that lipid dispersions in 50 mM Tris (pH 7.5) consisting of 50 wt % 22:6-22:6PC/50 mol % [3α-^{2}H$_1$]cholesterol were in the lamellar phase over a 20−40 °C temperature range. ^{1}H-decoupled ^{31}P NMR spectra recorded at 20, 30, and 40 °C are shown in Figure 1. They consist of powder patterns characteristic of the lamellar phase (*33*). Specifically, there is a low-frequency shoulder and a high-frequency peak corresponding to the chemical shift $\sigma_{||}$ and $\sigma_\perp$ of the rapidly reorienting phosphocholine headgroup in bilayers with their normal respectively parallel and perpendicular to the magnetic field. The chemical shift anisotropy $\Delta\sigma_{CSA}$ (=$\sigma_{||} - \sigma_\perp$) of 44 ± 1 ppm measured at each temperature is comparable with values published for PCs in the lamellar liquid-crystalline phase (*35*). A diffuse peak near 0 ppm in the spectra at 30 and 40 °C (asterisks in Figure 1) indicates the presence of phospholipid structures in which motion is isotropic as temperature increases. It is a minor component,

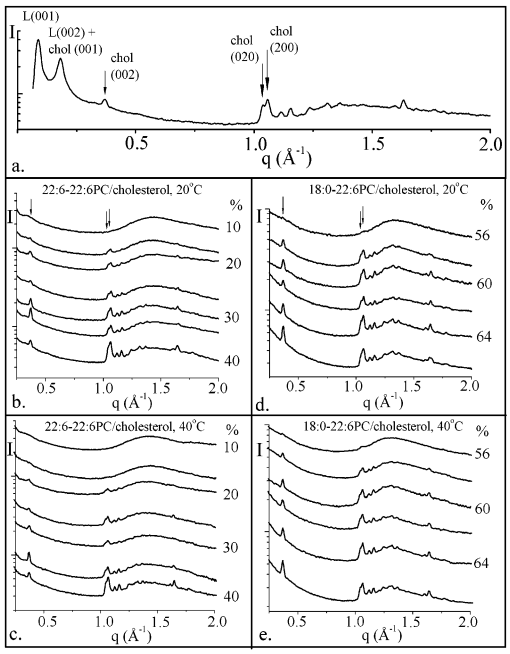

FIGURE 2: Integrated XRD radial intensity profiles for 50 wt % aqueous multilamellar dispersions in 50 mM Tris (pH 7.5) of (a) 22:6-22:6PC/40 mol % cholesterol at 20 °C, (b and c) 22:6-22:6PC/cholesterol at 20 and 40 °C, respectively, and (d and e) 18:0-22:6PC/cholesterol at 20 and 40 °C, respectively. The data shown in panel a cover the entire region of reciprocal space recorded, and reflections referred to in the text are labeled. These include the first [L(001)] and second [L(002)] low-angle lamellar reflections and the cholesterol monhydrate peaks [chol(002), chol(020), and chol(200)]. The plots shown in panels b−e have been cropped from $q = 0.25$ Å^{-1} to $q = 2.00$ Å^{-1} to focus on the wide-angle region used in quantifying cholesterol solubility. The q-space location of the (002), (020), and (200) cholesterol reflections are identified by arrows in panels b and d. Sterol concentration is indicated in mol %. The intensity scale is arbitrary and, to aid observation of weaker reflections, is logarithmic. Individual curves are shifted evenly along the intensity axis.

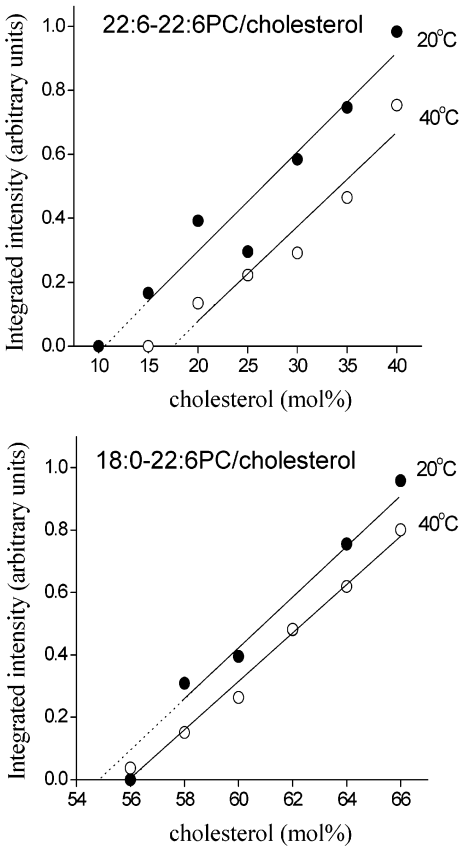

FIGURE 3: Dependence of the normalized diffracted intensity from cholesterol monohydrate on cholesterol concentration in 50 wt % aqueous multilamellar dispersions in 50 mM Tris (pH 7.5) of 22:6-22:6PC/cholesterol at 20 °C (●) and 40 °C (○) (upper panel) and 18:0-22:6PC/cholesterol at 20 °C (●) and 40 °C (○) (lower panel). Diffracted intensity was obtained as the sum of the (002), (020), and (200) cholesterol monohydrate reflections and was normalized with respect to the integrated intensity of the lipid wide-angle peak centered at $q \sim 1.4$ Å^{-1} (integration over q range 1.0−1.8 Å^{-1}). Linear fits to the data (solid lines) and extrapolations to the abscissa (dotted lines) are included.

amounting to <3% of the total integrated intensity of either spectrum, and will be neglected.

XRD. Additional confirmation that 22:6-22:6PC/cholesterol adopts lamellar phase under the conditions employed in this study was obtained from XRD measurements. The data in Figure 2a for a sample consisting of 22:6-22:6PC/40 mol % cholesterol at 20 °C show two low-angle peaks corresponding to the (001) and (002) reflections from the lamellar phase with a repeat spacing of $d_{001} \sim 70$ Å. This same pattern persisted at 30 and 40 °C (data not shown). No evidence for nonlamellar phases was observed.

The solubility of cholesterol in multilamellar dispersions of 22:6-22:6PC as opposed to 18:0-22:6PC was compared. To this end, low- and wide-angle XRD patterns were collected at 20 and 40 °C as a function of the concentration of cholesterol (χ_{chol}) added to samples hydrated to the extent of 50 wt % in Tris buffer (pH 7.5). Figure 2 shows plots of integrated radial intensity (I) vs reciprocal space ($q = 4\pi \sin\theta/\lambda$, where 2θ is the scattering angle and λ is the X-ray wavelength, 1.542 Å) ($I-q$ plots). The plots (Figure 2b−e) are cropped between $q = 0.25$ Å^{-1} and $q = 2.0$ Å^{-1} to focus on the region where peaks from crystalline cholesterol monohydrate appear when the solubility limit of the membrane is exceeded. As illustrated in Figure 2a, these peaks are observed at 0.37 Å^{-1} ($d = 17$ Å), 1.03 Å^{-1} ($d = 6.08$ Å), and 1.04 Å^{-1} ($d = 6.02$ Å), corresponding to the 002, 020, and 200 reflections (*28*). Although the 020 and 200 peaks overlap, they are resolvable as two separate peaks during the fitting procedure.

Figure 2b shows $I-q$ plots for 22:6-22:6PC/cholesterol multilamellar dispersions at 20 °C where the cholesterol content is varied from 10 to 40 mol % in 5 mol % increments. Inspection of the plots reveals that second-order reflections from cholesterol monohydrate were present when $\chi_{chol} = 15$ mol % and grew in intensity as χ_{chol} was increased. They were not observed with 10 mol % cholesterol. At 40 °C, the behavior was qualitatively similar but indicative of slightly higher membrane solubility for cholesterol (Figure 2c). Specifically, the peaks from solid sterol did not appear until a concentration of 20 mol % was reached and then grew in intensity as χ_{chol} increased. The telltale reflections were absent at 10 and 15 mol % cholesterol.

The normalized and summed integrated intensities of the three second-order diffraction peaks from cholesterol monohydrate in Figure 2b,c are plotted against cholesterol concentration in Figure 3 (upper panel). A linear extrapolation to zero integrated intensity of the data for 20 °C intercepts the abscissa at 11 ± 3 mol % cholesterol (filled

circles). This intercept represents the solubility limit of cholesterol as determined by XRD, χ_{chol}^{XRD}, in 22:6-22:6PC bilayers at this temperature. The failure to detect diffraction peaks from solid cholesterol in 22:6-22:6PC when 10 mol % was present lends further credence to the determination (Figure 2b). The measurements performed at 40 °C (Figure 2c) were processed in the same way. From the intercept in Figure 3 (upper panel), the solubility of cholesterol in this system was found to rise to a value of 17 ± 3 mol % at 40 °C (open circles). The solubility limits just described did not change upon incubating samples for >12 h (data not shown). Furthermore, the solubility was seen to drop to its original low-temperature value when the sample was cooled from 40 to 20 °C (Brzustowicz, Zerouga, Cherezov, Caffrey, Stillwell, and Wassall, unpublished). The solubility limits can be considered, thus, as representing equilibrium values.

I−*q* plots for the control system consisting of 18:0-22:6PC and cholesterol, where the concentration of sterol was varied from 56 to 66 mol % in 2 mol % increments, are displayed in Figure 2d,e. At 20 °C, reflections from cholesterol monohydrate were barely perceptible at 56 mol % cholesterol. They did not appear with noticeable intensity until the cholesterol content reached 58 mol % and their intensity grew with increasing levels throughout the range studied up to 66 mol % cholesterol (Figure 2d). Similarly, cholesterol monohydrate peaks first became just discernible at $\chi_{chol} = 56$ mol % and then grew in intensity through $\chi_{chol} = 66$ mol % at 40 °C (Figure 2e). The normalized and summed integrated intensities of the three second-order reflections from cholesterol monohydrate in Figure 2d,e are plotted against cholesterol concentration in Figure 3 (lower panel). Linear extrapolations to zero integrated intensity reveal the solubility limit as $\chi_{chol}^{XRD} = 55 \pm 3$ mol % at 20 °C (filled circles) and $\chi_{chol}^{XRD} = 56 \pm 3$ mol % at 40 °C (open circles). We conclude therefore that the membrane solubility of cholesterol in 18:0-22:6PC is high and, within experimental uncertainty, insensitive to temperature over the 20−40 °C range.

^{2}H NMR. The most probable orientation of [3α-^{2}H$_1$]-cholesterol incorporated into 22:6-22:6PC and 18:0-22:6PC bilayers was determined by ^{2}H NMR. Spectra recorded at 20, 30, and 40 °C for multilamellar dispesions of 22:6-22:6PC/50 mol % [3α-^{2}H$_1$]cholesterol hydrated to 50 wt % in Tris (pH 7.5) are shown in Figure 4a. The repetition rate (delay = 75 ms) between pulse sequences allows full recovery and detection of the signal from membrane-intercalated [3α-^{2}H$_1$]cholesterol which is characterized by a short spin−lattice relaxation time $T_1 \sim 3$ ms (*15*, *16*). In contrast, although XRD indicates that crystalline [3α-^{2}H$_1$]-cholesterol monohydrate is present, its much more slowly relaxing signal ($T_1 \sim 3$ s) was essentially completely attenuated and did not contribute to the spectra (*15*, *16*). The observation of an additional broad spectral component with a spliting $\Delta\nu_r \sim 120$ kHz in experiments run with a repetition time of 15 s, which was sufficient for relaxation of the solid to occur, confirmed this assessment (*15*, *16*). The central peak observed in the spectra is likely instrumental in origin, although it may be partially attributed to residual ^{2}HHO which persisted despite six exchanges with excess DDW. There may also be a minimal contibution from [3α-^{2}H$_1$]-cholesterol incorporated into an isotropic phospholipid phase

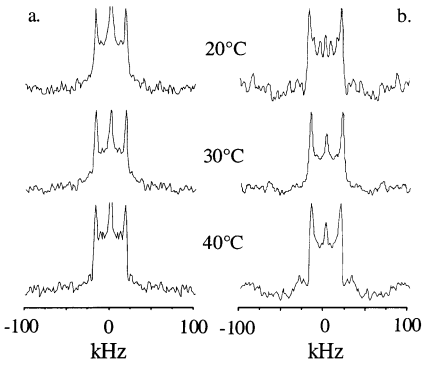

FIGURE 4: ^{2}H NMR spectra for 50 wt % aqueous multilamellar dispersions in 50 mM Tris (pH 7.5) at 20, 30, and 40 °C of (a) 22:6-22:6PC/50 mol % [3α-^{2}H$_1$]cholesterol and (b) 18:0-22:6PC/10 mol % [3α-^{2}H$_1$]cholesterol. Spectral parameters are as described in the text.

at the higher temperatures studied since, as mentioned earlier, the ^{31}P NMR spectra for 22:6-22:6/50 mol % [3α-^{2}H$_1$]-cholesterol at 30 and 40 °C (Figure 1) contained an isotropic signal of small intensity representing <3 mol % phospholipid.

In the spectrum recorded for 22:6-22:6PC/50 mol % [3α-^{2}H$_1$]cholesterol at 20 °C (Figure 4a) the signal comes from 11 mol % [3α-^{2}H$_1$]cholesterol, as determined by XRD, that intercalates into the membrane at this temperature. Axially symmetric, rapid reorientation of the steroid moiety about the bilayer normal reduces the quadrupolar splitting from the static value, $\Delta\nu_r = 120$ kHz, seen in solid sterol to the residual value measured $\Delta\nu_r = 35 \pm 1$ kHz. This splitting corresponds to an order parameter of $S_{CD} = 0.27$ (eq 1) from which a molecular order parameter $S_\alpha = 0.61$ (eq 2), characterizing the fluctuations in orientation of the long molecular axis of the steroid moiety relative to the bilayer normal, was calculated. Invoking a Gaussian distribution function of angles α (*25*), the most probable molecular orientation $\alpha_0 = 24° \pm 1°$ (eq 3) was then deduced. The spectra for 22:6-22:6PC/50 mol % [3α-^{2}H$_1$]cholesterol at 30 and 40 °C (Figure 4a) have identical quadrupolar splitting $\Delta\nu_r = 35 \pm 1$ kHz, which is indistinguishable from the value at 20 °C and implies that the tilt angle is independent of temperature in the range studied. Although XRD indicated that sterol intercalation within the dipolyunsaturated bilayers increased from 11 to 17 mol % when the temperature was increased from 20 to 40 °C, its orientation in the membrane is insensitive to temperature despite the rise in solubility.

We previously determined the tilt angle of [3α-^{2}H$_1$]-cholesterol intercalated to the extent of 50 mol % into 18:0-22:6PC membranes to be 16° ± 1° at 20 °C (*15*). This value is considerably less than the measurement of 24° ± 1° made in the current work for 22:6-22:6PC bilayers at the same temperature containing their solubility limit of 11 mol % sterol. To attain greater equivalence between the heteroacid saturated−polyunsaturated and homoacid dipolyunsaturated phospholipid systems for purposes of comparison, we reduced the amount of sterol added to 18:0-22:6PC to 10 mol %. ^{2}H NMR spectra for 18:0-22:6PC/10 mol % [3α-^{2}H$_1$]cholesterol are displayed as a function of temperature in Figure 4b. At 20 °C, a powder pattern with residual splitting $\Delta\nu_r = 39 \pm 1$ kHz was observed. The corresponding C−^{2}H bond and molecular order parameters are $S_{CD} = 0.30$

and $S_\alpha = 0.68$, respectively. They equate to a tilt angle $\alpha_0 = 21° \pm 1°$, identifying an increase of $4° \pm 2°$ in tilt angle relative to the value of $\alpha_0 = 17° \pm 1°$ obtained with 50 mol % incorporation of sterol into the mixed saturated−polyunsaturated chain membrane (Brzustowicz and Wassall, unpublished). The splitting measured for 18:0-22:6PC/10 mol % [3α-$^2H_1$]cholesterol at 30 °C was $\Delta\nu_r = 37 \pm 1$ kHz, on the basis of which order parameters $S_{CD} = 0.29$ and $S_\alpha = 0.65$, and tilt angle, $\alpha_0 = 22° \pm 1°$, were calculated. At 40 °C, the splitting was reduced further to $\Delta\nu_r = 35 \pm 1$ kHz. The corresponding order parameters are $S_{CD} = 0.27$ and $S_\alpha = 0.61$, and the equivalent tilt angle is $\alpha_0 = 24° \pm 1°$.

DISCUSSION

Phase Behavior. Previous reports have noted that dipolyunsaturated PC systems may form nonbilayer phases (*21*, *22*). In this study, we established that fully hydrated dispersions composed of 22:6-22:6PC/50 mol % [3α-$^2H_1$]-cholesterol formed the lamellar phase at pH 7.5 in the temperature range from 20 to 40 °C. From the line shape of ^{1}H-decoupled ^{31}P NMR spectra shown in Figure 1, it was deduced that only lamellar phase existed at 20 °C while a relatively small amount (<3%) of isotropic structures appeared in addition to the predominant lamellar phase at 30 and 40 °C. The spectrum at 20 °C was a single-component powder pattern characteristic of lamellar phase ($\Delta\sigma_{CSA} = 44 \pm 1$ ppm), upon which a minor isotropic signal at 0 ppm became superimposed at 30 and 40 °C. In agreement with these observations, only lamellar phase was found for 22:6-22:6PC/50 mol % cholesterol at 25 °C in a separate ^{31}P NMR study (*20*). Our XRD data corroborate these findings. In the absence of cholesterol, lamellar phase alone was observed for 22:6-22:6PC by ^{31}P NMR between 20 and 50 °C (Brzustowicz and Wassall, unpublished), as is expected for PCs at physiological hydration, temperature, and pH (*35*).

Consistent with our observations, an earlier ^{31}P NMR study of 22:6-22:6PC reported the formation of only the lamellar phase at temperatures <60 °C. At temperatures >60 °C, an isotropic phase was observed that constituted the entire sample when 90 °C was reached (*21*). The addition of equimolar cholesterol resulted in the appearance of isotropic structures at 30 °C, and upon increasing the temperature to 60 °C nearly all of the sample existed in the inverted hexagonal (H_{II}) phase. On the basis of ^{2}H and ^{31}P NMR spectra, we also saw H_{II} and isotropic phases in 22:6-22:6PC/50 mol % [2,2,3,4,4,6-$^2H_6$]cholesterol at temperatures above 10 °C (*22*). The isotropic phases were later verified by XRD to be the cubic phases, *Ia*3*d* and *Pn*3*m* (Brzustowicz, Zerouga, Cherezov, Caffrey, Stillwell, and Wassall, unpublished). Nonlamellar phases, however, appeared only in samples with pH <5.0 where a minimum of 15 mol % cholesterol was necessary to induce the appearance of H_{II}, *Ia*3*d*, and *Pa*3m phases. Although it is apparent that cholesterol can induce 22:6-22:6PC to form nonlamellar phases, the conditions of low pH or high temperature required so far deviate appreciably from physiological. Future studies will determine whether the inclusion of ions or fusogenic molecules can cause these nonlamellar phases to be seen under biologically relevant conditions.

Cholesterol Solubility. Cholesterol may be incorporated into membranes up until a critical point after which the excess crystallizes outside of the membrane in monohydrate form. It has been generally assumed that ≥50 mol % cholesterol could be accommodated in phospholipid bilayers (*36*). Recently, studies have focused on determining solubility of the sterol as a function of headgroup and acyl chain composition (*15*, *16*, *26*). As high as 66 ± 1 mol % incorporation has been reported for 1,2-dilauroyl-*sn*-phosphatidylcholine (12:0-12:0PC), 1,2-dipalmitoyl-*sn*-phosphatidylcholine (16:0-16:0PC), 1-palmitoyl-2-oleoyl-*sn*-phosphatidylcholine (16:0-18:1PC), and 1,2-dierucyl-*sn*-phosphatidylcholine (22:1-22:1PC) membranes at 24 °C (*26*). On the basis of the detection of XRD diffraction peaks from crystals of cholesterol monohydrate which have phase separated from the membrane, in the current study we have established that the solubility of cholesterol at 20 °C is 11 ± 3 mol % for 22:6-22:6PC and 56 ± 3 mol % for 18:0-22:6PC (Figures 2 and 3). We observed a similar reduction in cholesterol solubility for homoacid dipolyunsaturated 20:4-20:4PC vs heteroacid saturated−polyunsaturated 18:0-20:4PC bilayers at 20 °C where respective solubility limits $\chi_{chol}^{XRD} = 15 \pm 2$ mol % and $\chi_{chol}^{XRD} \approx 50-55$ mol % were determined with the same method employed in this work (*16*). Combined, these studies demonstrate clearly that the presence of polyunsaturation at both *sn*-1 and *sn-2* positions dramatically reduces the solubility of cholesterol in hydrated PC bilayers to <20 mol %. The data further suggest that the solubility is less for the longer, more extensively unsaturated 22:6-22:6PC ($\chi_{chol}^{XRD} = 11 \pm 3$ mol %) than for 20:4-20:4PC ($\chi_{chol}^{XRD} = 15 \pm 2$ mol %), although the differential is not statistically significant. We surmise that the solubility of ∼55 mol % measured in 18:0-22:6PC and 18:0-20:4PC bilayers is symptomatic of preferential affinity of cholesterol for the saturated *sn*-1 chain, the polyunsaturated 20:4 or 22:6 acyl chain at the *sn*-2 position causing a decrease relative to the amount of sterol (∼66 mol %) that intercalates into PC membranes possessing no or one double bond per chain. Clearly, acyl chain polyunsaturation is a significancant factor in modulating cholesterol's ability to reside within a membrane.

The effects of temperature on cholesterol solubility were also investigated in the current work. When the temperature was raised from 20 to 40 °C, the solubility of cholesterol in 22:6-22:6PC increased from 11 ± 3 mol % to 17 ± 3 mol % (Figure 3, upper panel). The increase in solubility measured in the dipolyunsaturated system, albeit on the edge of experimental error, indicates that some of the phase-separated crystalline cholesterol monohydrate at 20 °C could be incorporated into the membrane with a rise in temperature. Upon cooling back to 20 °C the solubility returned to ∼11 mol % (data not shown). These data imply that the phase-separated sterol is in close proximity to the membrane to facilitate exchange between extra- and intramembrane environments. A similar assertion was made in a ^{2}H NMR study of *Acholeplasma laidlawii* membranes cultured in cholesterol-rich media where two pools of deuterated [2,2,3,4,6-$^2H_5$]-cholesterol, one dissolved in the membrane (≈10−15 mol % at 37 °C) and the other solidlike, were observed (*37*). Further incorporation into the biomembrane occurred when the temperature was raised, suggesting that sterol in the solid pool could gain ready access to the bilayer. Crystallization of excess cholesterol has been proposed to begin around the

headgroup region in 16:0-16:0PC membranes at mixing ratios of sterol/PC above their solubility limit (*38*). The proposal was inferred from a change in line shape of ^{31}P NMR spectra following the breakdown of crystalline cholesterol into submicroscopic crystals by sonication and freeze−thaw cycles. Without sonication and freeze−thaw cycling, as in the present study, the line shape was unaffected by the presence of large crystals outside the bilayer.

In another study, crystalline cholesterol that was initially excluded from 16:0-18:1PC bilayers was seen by optical microscopy to be absorbed after incubation (*26*). The apparent solubility grew from 52 mol % to about 57 mol % or 60 mol % when sample sets were incubated for 1 month at 25 or 40 °C, respectively. This change was attributed to partial remixing of sterol that had demixed from phospholipid when the sample was passed through an intermediate dry state during preparation. We consider that such artifactual crystallization of cholesterol is responsible for neither the low solubility in 22:6-22:6PC bilayers seen in the current work nor its increase at higher temperature. The solubility experiments described here were performed on samples that were lyophilized at low temperature to trap the lipids in a well-mixed state. Our observation that solubility in 22:6-22:6PC bilayers returned to the value originally measured when the sample was cooled back to 20 °C is also inconsistent with remixing of cholesterol that had been excluded while the samples were prepared. Moreover, there is essentially no change in the solubility that we measured for cholesterol in 18:0-22:6PC membranes heated from 20 °C ($\chi_{chol}^{XRD} = 55 \pm 3$ mol %) to 40 °C ($\chi_{chol}^{XRD} = 56 \pm 3$ mol %) (Figure 3, lower panel). These findings indicate that demixing of sterol from phospholipid is not a problem during the preparation of highly unsaturated samples. Additional support for this assertion is derived from our previous investigation which found that the solubility measured in 20:4-20:4PC membranes prepared by the low-temperature trapping method agreed with the value obtained with samples prepared in the conventional manner (*16*).

Lateral Organization and Solubility. A recent theory proposes a link between the lateral organization of cholesterol within a membrane and its solubility therein (*27*). The molecular basis is the assignment of a highly unfavorable energy to cholesterol multibody interactions. To mimimize cholesterol−cholesterol contacts, highly regular distributions of lipid possessing rectangular or hexagonal symmetry are formed at critical sterol/phospholipid molar ratios. A steep jump in cholesterol potential energy that favors precipitation from the bilayer then accompanies a slight increase in sterol content because the phospholipid polar headgroups (acting as "umbrellas") can no longer sufficiently shelter membrane-intercalated sterol from interfacial waters. Monte Carlo simulations identified three critical cholesterol mole fractions at 50, 57, and 67 mol %. The highest value is in close agreement with the solubility of 66 mol % reported for 12:0-12:0PC, 16:0-16:0PC, 16:0-18:1PC, and 22:1-22:1PC bilayer systems containing saturated or monounsaturated chains (*26*), while the solubility of ∼56 mol % in *sn*-1 saturated *sn*-2 polyunsaturated 18:0-22:6PC bilayers from our work coincides well with the intermediate value. Although the multibody interaction treatment was not extended to low (<20 mol %) cholesterol content, the solubility of 10−20 mol % determined in dipolyunsaturated 22:6-22:6PC bilayers may be qualitatively reconciled in terms of the umbrella model. The molecular area of dipolyunsaturated PCs is substantially greater than PCs possessing a saturated chain (*39*), resulting in less effective shielding by the headgroups and a greater likelihood of exposure to water for membrane-intercalated sterol. Subsequent exclusion from the membrane via the formation of cholesterol monohydrate crystals would, thus, be promoted at low cholesterol concentrations. In support of this explanation, highly polyunsaturated bilayers are significantly more permeable to water than less unsaturated bilayers (*40*) which would facilitate more frequent close contact of water with molecules therein.

Models invoking the regular distribution of lipids at low concentration of sterol have also been put forward (*41*, *42*). In particular, the formation of hexagonal superlattices achieving maximal separation between cholesterol molecules within 1,2-dimyristoyl-*sn*-phosphatidylcholine (14:0-14:0PC) bilayers has been predicted for specific concentrations which include 10, 11.8, 14.3, 15.4, and 20 mol % sterol (*42*). These values encompass the solubility determined here in 22:6-22:6PC membranes, and it is tempting to speculate that the solubility limit corresponds to a highly organized lateral array of cholesterol within the dipolyunsaturated system. However, we emphasize that such an arrangement should not be viewed as static in liquid-crystalline membranes characterized by rapid lateral mobility. The concept envisaged by the superlattice model has the coexistence of dynamic regions of limited size in which molecules are regularly distributed (*41*, *42*).

Cholesterol Molecular Orientation. The motion of cholesterol intercalated into a membrane is a composite that consists of discrete restricted jumps about its long molecular axis and libration or "wobbling" of this axis about the bilayer normal. Invoking a population-weighted Gaussian function to describe the distribution of angles α made with respect to the bilayer normal (eq 3), the libration may then be characterized by a tilt angle α_0 which represents the most probable orientation of the steroid moiety (*15*, *16*, *25*, *31*). This approach was adopted here to analyze ^{2}H NMR spectra recorded for aqueous dispersions of 22:6-22:6PC/50 mol % [3α-^{2}H$_1$]cholesterol and 18:0-22:6PC/10 mol % [3α-^{2}H$_1$]-cholesterol (Figure 4). The tilt angles α_0 obtained and their variation with temperature are summarized in Figure 5. Included in the graph are data for 18:0-22:6PC/50 mol % [3α-^{2}H$_1$]cholesterol at 20 °C (*15*) and at 30 and 40 °C (Brzustowicz and Wassall, unpublished).

Figure 5 shows that at 20 °C the tilt angle in 22:6-22:6PC/50 mol % [3α-^{2}H$_1$]cholesterol ($\alpha_0 = 24° \pm 1°$) is substantially bigger than in 18:0-22:6PC/50 mol % [3α-^{2}H$_1$]-cholesterol ($\alpha_0 = 17° \pm 1°$). The same disparity in sterol orientation was seen between 20:4-20:4PC/50 mol % [3α-^{2}H$_1$]cholesterol and 18:0-20:4PC/50 mol % [3α-^{2}H$_1$]cholesterol at 20 °C (*16*). The identical tilt angles measured in the heteroacid saturated−polyunsaturated phospholipids reflect an earlier noted insensitivity to the degree of unsaturation at the *sn*-2 position when the *sn*-1 chain is saturated (*15*, *16*). A review of the literature illustrates that $\alpha_0 = 16° \pm 1°$ applies to equimolar [3α-^{2}H$_1$]cholesterol in 16:0-16:0PC, 1-stearoyl-2-oleoyl-*sn*-phosphatidylcholine (18:0-18:1PC), egg PC, 18:0-20:4PC, and 18:0-22:6PC membranes (*15*, *31*, *43*). As our XRD experiments indicated that only 11 ± 3

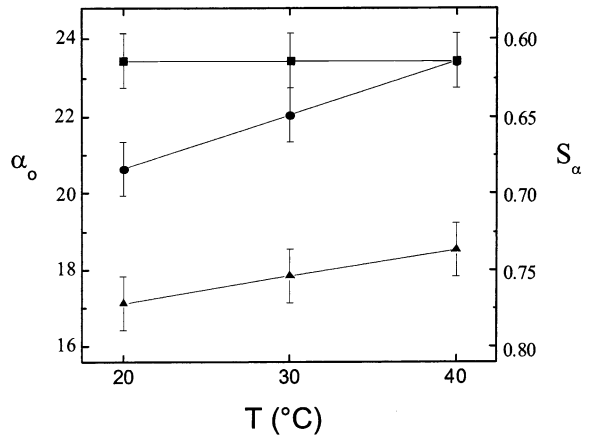

FIGURE 5: Temperature dependence of the tilt angle α_0 and molecular order parameter S_α for membrane-intercalated [3α-$^2H_1$]-cholesterol in 50 wt % aqueous multilamellar dispersions in 50 mM Tris (pH 7.5) of 22:6-22:6PC/50 mol % [3α-$^2H_1$]cholesterol (■) and 18:0-22:6PC/10 mol % [3α-$^2H_1$]cholesterol (●). Data for 18:0-22:6PC/50 mol % [3α-$^2H_1$]cholesterol (▲) are included for comparison (Brzustowicz and Wassall, unpublished). It should be noted that the values quoted in the text for α_0 and its uncertainty have been rounded off to two significant figures and ±1°, respectively.

mol % of the 50 mol % [3α-$^2H_1$]cholesterol added to 22:6-22:6PC will incorporate into the membrane at 20 °C (Figure 3, upper panel), 18:0-22:6PC/10 mol % [3α-$^2H_1$]cholesterol bilayers containing a comparable amount of intercalated sterol constitute a more meaningful comparison. Specifically, a somewhat larger tilt angle relative to membranes containing 50 mol % cholesterol is to be expected since a lower concentration of sterol will order the host membrane less facilitating greater freedom for molecular reorientation therein (*25*, *31*, *43*). The tilt angle $\alpha_0 = 21° \pm 1°$ determined in 18:0-22:6PC/10 mol % [3α-$^2H_1$]cholesterol membranes at 20 °C exhibits the anticipated increase but is still smaller than in the dipolyunsaturated system at the same temperature.

Inspection of Figure 5 further reveals that the molecular orientation of [3α-$^2H_1$]cholesterol in 22:6-22:6PC membranes responds differently to changes in temperature than in 18:0-22:6PC. The tilt angle in 22:6-22:6PC/50 mol % [3α-$^2H_1$]-cholesterol remained constant ($\alpha_0 = 24° \pm 1°$) when the temperature was raised from 20 to 40 °C, whereas there were increases in 18:0-22:6PC/10 mol % [3α-$^2H_1$]cholesterol ($\alpha_0 = 21° \pm 1°$ to $\alpha_0 = 24° \pm 1°$) and 18:0-22:6PC/50 mol % [3α-$^2H_1$]cholesterol ($\alpha_0 = 17° \pm 1°$ to $\alpha_0 = 19° \pm 1°$) over this temperature range. The modest rise in amplitude of sterol libration seen with the mixed saturated−polyunsaturated chain phospholipid is consistent with the behavior reported for less unsaturated systems possessing a saturated *sn*-1 chain (*25*, *31*, *43*). Greater disorder within the host membrane at higher temperature is responsible. The contrasting absence of a response to temperature from α_0 for [3α-$^2H_1$]cholesterol in dipolyunsaturated 22:6-22:6PC suggests that molecular ordering within the dipolyunsaturated membrane is unaffected. Perhaps, the additional intercalation of sterol into the membrane at higher temperature identified by XRD causes a compensatory increase in order to offset any temperature-associated decrease in order.

Saturated vs Polyunsaturated Acyl Chains. We attribute the greatly reduced solubility of cholesterol seen in 22:6-22:6PC vs 18:0-22:6PC, and 20:4-20:4PC vs 18:0-20:4PC (*16*), to a fundamental difference between the molecular organization of saturated and polyunsaturated acyl chains. ^2H NMR data indicate that cholesterol's effect on the order of the saturated *sn*-1 chain in mixed-chain PC bilayers changes little in the presence of polyunsaturation at the *sn*-2 position. A qualitatively similar increase in orientational order for the saturated [$^2H_{31}$]palmitoyl ([$^2H_{31}$]16:0) *sn*-1 chain was observed upon incorporation of cholesterol into liquid-crystalline [$^2H_{31}$]16:0-20:4PC, 1-[$^2H_{31}$]palmitoyl-2-linoleoylphosphatidylcholine ([$^2H_{31}$]16:0-18:2PC), [$^2H_{31}$]16:0-18:1PC, and [$^2H_{31}$]16:0-16:0PC bilayers (*44*−*47*). The sterol acts predominantly by uniformly ordering the plateau region of approximately constant order in the upper portion of the acyl chain, and has progressively less effect in the lower region where order decreases toward the highly disordered terminal methyl group. Our interpretation is that the mostly all-trans configuration of the upper portion of the saturated fatty acyl chain (*48*, *49*) produces a smooth molecular surface that favors insertion of cholesterol into the membrane because it would be compatible with the rotational motion of a neighboring rigid rodlike sterol molecule. In addition, sterol motion parallel to the bilayer normal would be facilitated. Out-of-plane diffusion has been included in theoretical treatments of the interaction of cholesterol with lipid bilayers (*50*) and was assigned an amplitude of >5 Å in neutron scattering experiments on l_o phase 16:0-16:0PC (*51*).

The order and dynamics of polyunsaturated acyl chains in the presence of cholesterol have not been elucidated to date. Time-resolved fluorescence of 1,6-diphenyl-1,3,5-hexatriene (DPH) showed that addition of 30 mol % sterol restricted molecular motion in homoacid dipolyunsaturated 22:6-22:6PC membranes much less than in its heteroacid saturated−polyunsatuarted counterpart 18:0-22:6PC (*52*), but provided no details of the motions undergone by the DHA chain. A highly disordered conformation has emerged as the consensus for polyunsaturated chains. Molecular models for 1,4-pentadiene gave initial insight. They revealed that, compared to the saturated bonds in *n*-pentane, there is a reduced energy barrier to rotational isomerization about the single C−C bonds which separate the unsaturated carbons atoms in PUFA (*53*). Compensation for the rigidity of the multiple double bonds is thus provided. Order parameter profiles generated from molecular dynamics simulations of 18:0-22:6PC bilayers (*11*, *13*) and 16:0-22:6PC bilayers (*12*) showed that, in complete contrast to the adjacent saturated *sn*-1 chain, the entire 22:6 chain possesses very low order parameters ($S_{CD} \approx 0-0.1$). The simulations indicated an extremely flexible structure for DHA in which rapid structural transitions occur between torsional states including extended and bent conformations. Experimental evidence supports high conformational flexibility. A ^{13}C and ^1H MAS NMR investigation of 16:0-22:6PC membranes demonstrated that the polyunsaturated chain approaches the membrane surface based on the detection of cross-peaks between the choline in the polar headgroup and the 22:6 chain in two-dimensional cross-polarization (CP) experiments (*54*). Rotating frame spin−lattice relaxation mesurements further indicate that methylene groups in the 22:6 chain undergo motions with correlation times in the 10^{-6} s range. Motionally narrowed, multicomponent ^2H NMR spectra observed for vinyl perdeuterated 16:0-[5,6,8,9,11,12,14,15-$^2H_8$]20:4PC (*55*) and 16:0-[4,5,7,8,10,11,13,14,16,17,19,20-$^2H_{12}$]22:6PC

(*56*) membranes and newly reported ^{2}H NMR data on perdeuterated 18:0-[$^2H_{31}$]22:6PC (*57*), moreover, are consistent with high disorder for the polyunsaturated acyl chains.

We propose that the highly disordered state of DHA chains is incompatible with close proximity to a rigid steroid moiety. The considerable restriction to reorientation of the chain that would ensue if cholesterol were to come into intimate contact would be entropically unfavorable. Unlike saturated chains, the polyunsaturated acyl chain also does not provide a smooth facade conducive to the motions likely to be performed within the membrane by a nearby sterol molecule. Neither rapid rotation about the long molecular axis nor fluctuations parallel to the bilayer normal would be facilitated. Our proposal explains the low solubility of cholesterol (<20 mol %) measured in 22:6-22:6PC or 20:4-20:4PC membranes. To avoid proximity to polyunsaturated chains at both *sn*-1 and *sn*-2 positions, sterol is excluded from the membrane. In 18:0-22:6PC or 18:0-20:4PC membranes, cholesterol would preferentially associate with the saturated chain at the *sn*-1 position. The presence of *sn*-2 polyunsaturation causes a minimal reduction in solubility (~55 mol % vs 66 mol %) relative to disaturated and other less unsaturated phospholipids. In support, ^{1}H MAS NMR experiments on 18:0-22:6PC/50 mol % [25,26,26,26,27,27,27-$^2H_7$]cholesterol membranes revealed closer contact with the 18:0 *sn*-1 chain than with DHA at the *sn*-2 position via a higher rate of chain-to-cholesterol NOESY cross-relaxation (*20*).

Membrane Architecture. A propensity for cholesterol and PUFA to laterally phase separate into patches to avoid intimate contact in a membrane is implied by their low mutual affinity. Sterol-induced sorting of lipids in this manner has been hypothesized to promote the formation of PUFA-rich/cholesterol-poor and PUFA-poor/cholesterol-rich microdomains within cell membranes (*4*, *20*, *52*). Although unequivocal evidence is yet to be presented, data in favor of the hypothesis is becoming increasingly convincing. In an earlier study, we investigated [3α-$^2H_1$]cholesterol added to 20:4-20:4PC/18:0-20:4PC (1/1 mol) membranes (*16*). We were able to analyze the ^{2}H NMR spectrum recorded in terms of a model in which diffusion-mediated fast exchange of deuterated cholesterol occurs between 20:4-20:4PC/sterol-poor and 18:0-20:4PC/sterol-rich microdomains <160 Å in size. It has recently been reported, moreover, that model ROS disk membranes containing l_d domains composed of 22:6-22:6PC and l_o domains composed of 16:0-16:0PC/cholesterol were necessary to support optimal rhodopsin function (*58*). The hydrophobic thickness of l_d vs l_o domains is expected to be reduced, presumably matching the hydrophobic region of the protein.

In the best developed model for the interaction of cholesterol with PUFA, the function of rhodopsin in the ROS was linked to the presence of membrane−DHA (*52*, *59*, *60*). Primary control of rhodopsin activation was ascribed to the DHA acyl chain composition of phospholipids with secondary regulation by cholesterol content. An extension of this model has phase separation of l_d domains comprised of 22:6-22:6PC from l_o domains comprised of 16:0-16:0/cholesterol (*52*). Our description of the molecular sorting of lipids into 22:6-22:6PC-rich/cholesterol-poor l_d phases and saturated lipid-rich/cholesterol-rich l_o phases is depicted in Figure 6a, which represents a cartoon of an apical disk membrane leaflet. Here, the photoreceptor benefits from the unique

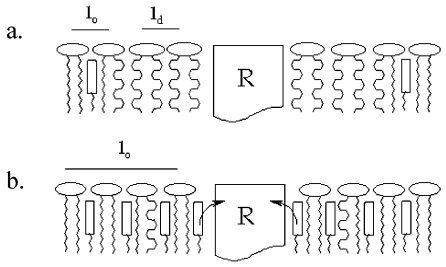

FIGURE 6: Cartoon depiction of neural tissue membranes. (a) Leaflet of a membrane where the PUFA-rich l_d phase excludes cholesterol and, as a result, facilitates receptor (R) function. This model would apply to rhodopsin in apical ROS membranes. (b) Leaflet of a membrane where the cholesterol-rich l_o domain facilitates access of cholesterol to receptor (R) and subsequent binding as indicated by arrows. This model would describe the activation of nAchR in nAchR-rich membranes or the inhibition of rhodopsin in basal ROS membranes.

micromechanical properties of a 22:6-22:6PC-rich l_d phase while maintaining a cholesterol-depleted environment necessary for activation (*61*). In contrast to apical ROS membranes, synaptic membranes rich in nAchR contain large quantities of saturated PC and cholesterol (*18*). Most of the polyunsaturated acyl chains are esterified to PS and PE. The anticipated abundance of l_o domains would facilitate the binding of cholesterol to receptor and consequent activation (*62*). The situation is depicted in Figure 6b in a cartoon representation of the nAchR-rich leaflet. Cholesterol would freely diffuse between l_d and l_o domains, driven by its affinity for saturated acyl chains. An analogous scenario may also contribute to the inhibition of rhodopsin in basal disk membranes where the concentration of cholesterol is substantially elevated (30 vs 5 mol %) relative to apical disk membranes (*63*). High cholesterol content impairs the function of rhodopsin (*61*), and direct interaction between sterol and receptor has been demonstrated (*64*). Mediation of rhodopsin function by a cholesterol-associated reduction in acyl chain packing free volume is an alternative mechanism that could apply to our model (*65*).

CONCLUSION

Our XRD and solid-state ^{2}H NMR results establish that the molecular organization of cholesterol differs markedly in 22:6-22:6PC and 18:0-22:6PC bilayers. In particular, the inability of cholesterol to intercalate into 22:6-22:6PC membranes in amounts comparable to 18:0-22:6PC membranes demonstrates the remarkable consequence of forcing a steric interaction between the rigid steroid moiety and the DHA chains at both *sn*-1 and *sn*-2 positions in the dipolyunsaturated bilayer. We propose that the high degree of disorder possessed by the polyunsaturated chain deters close proximity to the sterol which is then tolerated to a low level in the membrane. In contrast, the smooth facade presented by the predominantly all-trans configuration adopted by the upper portion of the saturated chain at the *sn*-1 position is favorable to near approach of the sterol and facilitates its intercalation into the saturated−polyunsaturated 18:0-22:6PC bilayer in large amounts.

The work presented here offers a plausible mechanism for cholesterol-induced sorting of membrane lipids into microdomains. Although lateral heterogeneity in the composition of cell membranes is unlikely to be entirely attributable to

lipid−lipid interactions, our model membrane study nonetheless attests to a strong preference for cholesterol to phase separate from regions rich in PUFA. Dipolyunsaturated 22:6-22:6PC model membranes represent an extreme in PUFA content. Insight gained from their study, in unison with knowledge on saturated lipid/cholesterol complexes (e.g., sphingolipid/cholesterol rafts), serves as a reference point in elucidating the role played by the myriad of lipids that work in concert within membranes to maintain an environment appropriate to cellular functioning.

ACKNOWLEDGMENT

We are grateful for the assistance of Dr. Stephanie Sen (IUPUI) in the synthesis and purification of [3α-$^2H_1$]-cholesterol.

REFERENCES

1. Salem, N., Jr., Kim, H.-Y., and Yergey, J. A. (1986) Docosahexaenoic acid: membrane function and metabolism, in *Health Effects of Polyunsaturated Fatty Acids in Seafoods* (Simopoulos, A. P., Kifer, R. R., and Martin, R. E., Eds.) pp 263−317, Academic Press, New York.
2. Salem, N., Jr., and Niebylski, C. D. (1995) The nervous system has an absolute molecular species requirement for proper function, *Mol. Membr. Biol. 12*, 131−134.
3. Bloom, M., Linseisen, F., Lloyd-Smith, J., and Crawford, M. (1999) Insights from NMR on the functional role of polyunsaturated lipids in the brain, in *Proceedings of the International School of Physics 'Enrico Fermi', Course CXXXIX on Magnetic Resonance and Brain Function: Approaches from Physics* (Maraviglia, B., Ed.) pp 527−553, IOS Press, Ohmsha.
4. Stillwell, W. (2000) Docosahexaenoic acid and membrane lipid domains, *Curr. Org. Chem. 4*, 1169−1183.
5. Brown, R. E. (1998) Sphingolipid organization in biomembranes: what physical studies of model membranes reveal, *J. Cell Sci. 111*, 1−9.
6. Simons, K., and Ikonen, E. (1997) Functional rafts in cell membranes, *Nature 387*, 569−572.
7. Gennis, R. B. (1989) *Biomembranes*, Springer-Verlag, New York.
8. McMullen, T. P. W., and McElhaney, R. N. (1996) Physical studies of cholesterol-phospholipid interactions, *Curr. Opin. Colloid Interface Sci. 1*, 83−90.
9. Finegold, L., Ed. (1993) *Cholesterol in Membrane Models*, CRC Press, Boca Raton, FL.
10. Ipsen, J. H., Karlstrom, G., Mouritsen, O. G., Wennerstrom, H., and Zuckermann, M. J. (1987) Phase equilibria in the phosphatidylcholine-cholesterol system, *Biochim. Biophys. Acta 905*, 162−172.
11. Saiz, L., and Klein, M. L. (2001) Structural properties of a highly polyunsaturated lipid bilayer from molecular dynamics simulations, *Biophys. J. 81*, 204−216.
12. Huber, T., Rajamoorthi, K., Kurze, V. F., Beyer, K., and Brown, M. F. (2002) Structure of docosahexaenoic acid-containing phospholipid bialyers as studied by ^2H NMR and molecular dynamics simulations, *J. Am. Chem. Soc. 124*, 298−309.
13. Feller, S. E., Gawrisch, K., and MacKerrell, A. D., Jr. (2002) Polyunsaturated fatty acids in lipid bilayers: intrinsic and environmental contributions to their unique physical properties, *J. Am. Chem. Soc. 124*, 318−326.
14. Aveldano, M. I. (1989) Dipolyunsaturated species of retina phospholipids and their fatty acids, *Colloq. INSERM 195*, 87−96.
15. Brzustowicz, M. R., Stillwell, W., and Wassall, S. R. (1999) Molecular organization of cholesterol in polyunsaturated phospholipid membranes: a solid state ^2H NMR investigation, *FEBS Lett. 451*, 197−202.
16. Brzustowicz, M. R., Cherezov, V., Caffrey, M., Stillwell, W., and Wassall, S. R. (2002) Molecular organization of cholesterol in polyunsaturated membranes: microdomain formation, *Biophys. J. 82*, 285−298.
17. Breckenridge, W. C., Morgan, I. G., Zanetta, J. P., and Vincedon, G. (1973) Adult rat brain synaptic vesicles. II. Lipid composition, *Biochim. Biophys. Acta 176*, 681−686.
18. Rotstein, N. P., Arias, H. R., Barrantes, F. J., and Aveldano, M. I. (1987) Composition of lipids in elasmobranch electric organ and acetylcholine receptor membranes, *J. Neurochem. 49*, 1333−1340.
19. Albert, A. D., Young, J. E., and Paw, Z. (1998) Phospholipid fatty acyl spatial distribution in bovine rod outer segment disk membranes, *Biochim. Biophys. Acta 1368*, 52−60.
20. Huster, D., Arnold, K., and Gawrisch, K. (1998) Influence of docosahexaenoic acid and cholesterol on lateral lipid organization in phospholipid mixtures, *Biochemistry 37*, 17299−17308.
21. Dekker, C. J., Geurts van Kessel, W. S. M.,. Klomp, J. P. G., Pieters J., and de Kruijff, B. (1983) Synthesis and polymorphic phase behavior of polyunsaturated phosphatidylcholines and phosphatidylethanolamines, *Chem. Phys. Lipids 33*, 93−106.
22. Brzustowicz, M. R., Zerouga, M., Cherezov, V., Caffrey, M., Stillwell, W., and Wassall, S. R. (2000) Solid-state NMR and X-ray diffraction studies of cholesterol molecular organization in polyunsaturated phospholipid bilayers, *Biophys. J. 78*, 184A.
23. Burger, K., Glimp, G., and Fahrenholz, F. (2000) Regulation of receptor function by cholesterol, *Cell. Mol. Life Sci. 57*, 1577−1592.
24. Zerouga, M., Jenski, L. J., and Stillwell, W. (1995) Comparison of phosphatidylcholines containing one or two docosahexaenoic acyl chains on properties of phospholipid monlayers and bilayers, *Biochim. Biophys. Acta 1236*, 266−272.
25. Oldfield, E., Meadows, M., Rice, D., and Jacobs, R. (1978) Spectroscopic studies of specifically deuterium labeled membrane systems. Nuclear magnetic resonance investigation of the effects of cholesterol in model systems, *Biochemistry 17*, 2727−2739.
26. Huang, J., Buboltz, J. T., and Feigenson, G. W. (1999) Maximum solubility of cholesterol in phosphatidylcholine and phosphatidylethanolamine bilayers, *Biochim. Biophys. Acta 1417*, 89−100.
27. Huang, J., and Feigenson, G. W. (1999) A microscopic interaction model of maximum solubility of cholesterol in lipid bilayers, *Biophys. J. 76*, 2142−2157.
28. Craven, B. M. (1976) Crystal structure of cholesterol monohydrate, *Nature 260*, 727−729.
29. McCabe, M. A., and Wassall, S. R. (1997) Rapid deconvolution of NMR powder spectra by weighted fast Fourier transformation, *Solid State Nucl. Magn. Reson. 10*, 53−61.
30. Davis, J. H., Jeffrey, K. R., Bloom, M., Valic, M. I., and Higgs, T. P. (1976) Quadrupolar echo deuteron magnetic resonance spectroscopy in ordered hydrocarbon chains, *Chem. Phys. Lett. 42*, 390−394.
31. Murari, R., Murari, M. P., and Baumann, W. J. (1986) Sterol orientations in phosphatidylcholine liposomes as determined by deuterium NMR, *Biochemistry 25*, 1062−1067.
32. Taylor, M. G., Akiyama, T., and Smith, I. C. P. (1981) The molecular dynamics of cholesterol in bilayer membranes: a deuterium NMR study, *Chem. Phys. Lipids 29*, 327−339.
33. Seelig, J. (1978) ^{31}P nuclear magnetic resonance and the head group structure of phospholipids in membranes, *Biochim. Biophys. Acta 515*, 105−140.
34. Rance, M., and Byrd, R. A. (1983) Obtaining high-fidelity spin-1/2 powder spectra in anisotropic media: phase-cycled Hahn echo spectroscopy, *J. Magn. Reson. 52*, 221−240.
35. Tilcock, C. P. S. (1986) Lipid polymorphism, *Chem. Phys. Lipids 40*, 109−125.
36. Phillips, M. C. (1990) Cholesterol packing, crystallization and exchange properties in phosphatidylcholine vesicles, *Hepatology 12*, 75S−82S.
37. Monck, M. A., Bloom, M., Lafleur, M., Lewis, R. N. A. H., McElhaney, R. N., and Cullis, P. R. (1993) Evidence for two pools of cholesterol in the *Acholeplasma laidlawii* strain B membrane: a deuterium NMR and DSC study, *Biochemistry 32*, 3081−3088.
38. Guo, W., and Hamilton, J. A. (1995) A multinuclear solid-state NMR study of phospholipid-cholesterol interactions. Dipalmitoylphosphatidylcholine-cholesterol binary system, *Biochemistry 34*, 14174−14184.
39. Smaby, J. M., Momsen, M. M., Brockman, H. L., and Brown, R. E. (1997) Phosphatidylcholine acyl unsaturation modulates the decrease in interfacial elasticity induced by cholesterol, *Biophys. J. 73*, 1492−1505.
40. Huster, D., Jin, A. J., Arnold, K., and Gawrisch, K. (1997) Water permeability of polyunsaturated lipid membranes measured by ^{17}O NMR, *Biophys. J. 73*, 855−864.
41. Chong, P. L.-G. (1994) Evidence for regular distribution of sterols in liquid crystalline phosphatidylcholine bilayers, *Proc. Natl. Acad. Sci. U.S.A. 91*, 10069−10073.

42. Virtanen, J. A., Ruonala, M., Vauhkonen, M., and Somerharju, P. (1995) Lateral organization of liquid-crystalline cholesterol−dimyristoylphosphatidylcholine bilayers. Evidence for domains with hexagonal and centered rectangular cholesterol superlattices, *Biochemistry 34*, 11568−11581.
43. Taylor, M. G., Akiyama, T., Saito, H., and Smith, I. C. P. (1982) Direct observation of cholesterol in membranes by deuterium NMR, *Chem. Phys. Lipids 31*, 359−379.
44. Vist, M. R., and Davis, J. H. (1990) Phase equilibria of cholesterol/dipalmitoylphosphatidylcholine mixtures: ^{2}H nuclear magnetic resonance and differential scanning calorimetry, *Biochemistry 29*, 451−464.
45. Thewalt, J. L., and Bloom, M. (1992) Phosphatidylcholine: cholesterol phase diagrams, *Biophys. J. 63*, 1176−1181.
46. Morrow, M. R., Davis, P. J., Jackman, C. S., and Keough, K. M. (1996) Thermal history alters cholesterol effect on transition of 1-palmitoyl-2-linoleoyl phosphatidylcholine, *Biophys. J. 71*, 3207−3214.
47. Jackman, C. S., Davis, P. J., Morrow, M. R., and Keough, K. M. W. (1999) Effect of cholesterol on the chain-ordering transition of 1-palmitoyl-2-arachidonoyl phosphatidylcholine, *J. Phys. Chem. B 103*, 8830−8836.
48. Schindler, H., and Seelig, J. (1975) Deuterium order parameters in relation to thermodynamic properties of a phospholipid bilayer. A statistical mechanical interpretation, *Biochemistry 14*, 2283−2287.
49. Douliez, J.-P., Leonard, A., and Dufourc, E. J. (1995) Restatement of order parameters in biomembranes: calculation of C−C bond order parameters from C−D quadrupolar splittings, *Biophys. J. 68*, 1727−1739.
50. Kessel, A., Ben-Tal, N., and May, S. (2001) Interactions of cholesterol with lipid bilayers: the preferred configuration and fluctuations, *Biophys. J. 81*, 643−658.
51. Gliss, C., Randel, O., Casalta, H., Sackmann, E., Zorn, R., and Bayerl, T. (1999) Anisotropic motion of choleserol in oriented DPPC bilayers studied by quasielastic neutron scattering: the liquid ordered phase, *Biophys. J. 77*, 331−340.
52. Mitchell, D. C., and Litman, B. J. (1998) Effect of cholesterol on molecular order and dynamics in highly polyunsaturated phospholipid bilayers, *Biophys. J. 75*, 896−908.
53. Applegate, K. R., and Glomset, J. A. (1986) Computer-based modeling of the conformation and packing properties of docosahexaenoic acid, *J. Lipid Res. 27*, 658−680.
54. Everts, S., and Davis, J. H. (2000) ^{1}H and ^{13}C NMR of multilamellar dispersions of polyunsaturated (22:6) phospholipids, *Biophys. J. 79*, 885−897.
55. Rajamoorthi, K., and Brown, M. F. (1991) Bilayers of arachidonic acid containing phospholipids studied by ^{2}H and ^{31}P NMR spectroscopy, *Biochemistry 30*, 4204−4212.
56. Dratz, E. A., and Deese, A. J. (1986) The role of docosahexaenoic acid (22:6ω3) in biological membranes: examples from photoreceptors and model membrane bilayers, in *Health Effects of Polyunsaturated Fatty Acids in Seafoods* (Simopoulos, A. P., Kifer, R. R., and Martin, R. E., Eds.) pp 319−351, Academic Press, New York.
57. Gawrisch, K., Eldho, N. V., Mathews, J. S., and Lindsay, C. C. (2002) The order parameter profile of docosahexaenoic acid in 18:0−22:6(d31)PC, *Biophys. J. 82*, 3a.
58. Polozova, A., and Litman, B. J. (2000) Cholesterol dependent recruitment of di22:6-PC by a G protein-coupled receptor into lateral domains, *Biophys. J. 79*, 2632−2643.
59. Mitchell, D. C., Straume, M., and Litman, B. J. (1992) Role of *sn*-1-saturated, *sn*-2-polyunsaturated phospholipids in control of membrane receptor conformational equilibrium: effects of cholesterol and acyl chain unsaturation on the Metarhodopsin I−Metarhodopsin II equilibrium, *Biochemistry 31*, 662−670.
60. Litman, B. J., and Mitchell, D. C. (1996) A role for phospholipid polyunsaturation in modulating membrane protein function, *Lipids 31*, S193−S197.
61. Boesze-Battaglia, K., and Albert, A. D. (1990) Cholesterol modulation of photoreceptor function in bovine retinal rod outer segments, *J. Biol. Chem. 265*, 20727−20730.
62. Addona, G. H., Sandermann, H., Kloczewiak, M. A., Husain, S. S., and Miller, K. W. (1998) Where does cholesterol act during activation of the nicotenic acetylcholine receptor?, *Biochim. Biophys. Acta 1370*, 299−309.
63. Boesze-Battaglia, K., Hennessey, T., and Albert, A. D. (1989) Cholesterol heterogeneity in bovine rod outer segment disk membranes, *J. Biol. Chem. 264*, 8151−8155.
64. Albert, A., Young, J. E., and Yeagle, P. L. (1996) Rhodopsin-cholesterol interactions in bovine rod outer segment disk membranes, *Biochim. Biophys. Acta 1285*, 47−55.
65. Niu, S.-L., Mitchell, D. C., and Litman, B. J. (2002) Manipulation of cholesterol levels in rod disk membranes by methyl-β-cyclodextrin, *J. Biol. Chem. 277*, 20139−20145.

BI0262808